

## MODELING AND CONTROL OF MULTI-LEVEL INVERTER FOR THREE-PHASE GRID-CONNECTED PHOTOVOLTAIC SOURCES

A. Jalilvand R. Noroozian M. Darabian

*Electrical Engineering Department, University of Zanjan, Zanjan, Iran*  
*ajalilvand@znu.ac.ir, noroozian@znu.ac.ir, m.darabian@znu.ac.ir*

**Abstract-** The paper deals with the multilevel converters control strategy for photovoltaic system integrated in distribution grids. The proposed control scheme ensures the injection of the generated power in the distribution grid with fast dynamic response, while providing an additional active power filtering capability providing the required harmonic and reactive currents to be considered. The control scheme is validated by means of simulations with a cascade converter which interfaces to a distribution grid. Also, for DC link voltage control, it is needed that stabilizes the voltage at the inverter input to insure a continuous flow of energy exchange between the grid and the PV system. Also, a LC filter is necessary to filter the output current and voltage from the harmonics and to protect the grid from their destructive effect. Finally, this paper presents detailed modeling of the grid-connected photovoltaic generation system components, in Simulink/Matlab software. Simulation results presented to validate the components models and the chosen control schemes.

**Keywords:** PV Generator, Inverter, Control Strategies, DC-DC Converter, PWM Inverter, MPPT, PI Controller.

### I. INTRODUCTION

Global warming and the limited resources of fossil fuels have increased the need for renewable energy [1-3]. Solar radiation is the largest source of renewable energy [4, 5] and the only one by which the present primary energy consumption can be replaced. Photovoltaic (PV) power generators convert the energy of solar radiation directly to electrical energy without any moving parts. PV power generators can be classified into stand-alone and grid-connected generators [6]. In recent years, there has been an increasing interest in the integration of Distributed Generation (DG) systems based on renewable energy resources to the distribution grid, which consider different objectives, such as technical [7], economical [8, 9], and environmental [10] aspects. It is estimated that the share of these resources (e.g., wind turbines, photovoltaic, fuel-cells, biomass, micro-turbines, small hydroelectric plants, and etc) in electrical networks will increase significantly in the near future [11, 12].

In parallel, the progress in technology has led to more powerful systems. Application of renewable energy resources in a power system may cause major changes in the design and operation of distribution grids [13]. Moreover, the environmental advantages, the shorter construction period can also be considered as a key driving element accelerating the development of DG technology [14].

Multilevel converters, are a good tradeoff solution between performance and cost in high-voltage and high-power systems. The main advantages of multilevel converters are reduced voltage ratings for the switches, good harmonic spectrum (making possible the use of smaller and less expensive filters), and good dynamic response [15]. However, the control complexity increases compared to conventional voltage source inverters (VSI). So, practical, cost effective, and flexible control strategies are vital to grid connection of renewable energy resources to the distribution grid.

Solar cells convert solar energy into electrical energy. This phenomenon occurs in materials which have the property of capture photon and emit electrons. The main material used in the photovoltaic industry is silicon. But there are many lines of research to find materials to replace or supplement to silicon to improve conversion efficiency, as for example [16, 17]. At present, photovoltaic generation is assuming increased importance as a renewable energy source application because of distinctive advantages such as simplicity of allocation, high dependability, absence of fuel cost, low maintenance and lack of noise and wear due to the absence of moving parts. The cell conversion ranges vary from 12% of efficiency up to a maximum of 29% for very expensive units [18]. In spite of those facts, there has been a trend in price decreasing for modern power electronics systems and photovoltaic cells, indicating good promises for new installations. However, the disadvantage is that photovoltaic generation is intermittent, depending upon weather conditions. Thus, the MPPT makes the PV system providing its maximum power and that energy storage element is necessary to help get stable and reliable power from PV system for both loads and utility grid, and thus improve both steady and dynamic behaviors of the whole generation system.

In this paper we have studied a grid-connected photovoltaic generation system which is composed of the PV array, power electronic converters, the filter, controllers, local loads and the utility grid as shown in Figure 1. The paper discusses the detailed modeling of the whole system. The PV array is connected to the utility grid by a boost converter to optimize the PV output and DC/AC inverter to convert the DC output voltage of the solar modules into the AC system. The DC input of the

inverter must be constant and it is controlled by the use of a PI controller. An LC filter has been introduced to insure a clean current injection to the grid. The proposed model of the entire components and control system are all simulated in Matlab/Simulink Software. Two different cases: steady and transient states are simulated, and all simulation results have verified the validity of models and effectiveness of control methods.

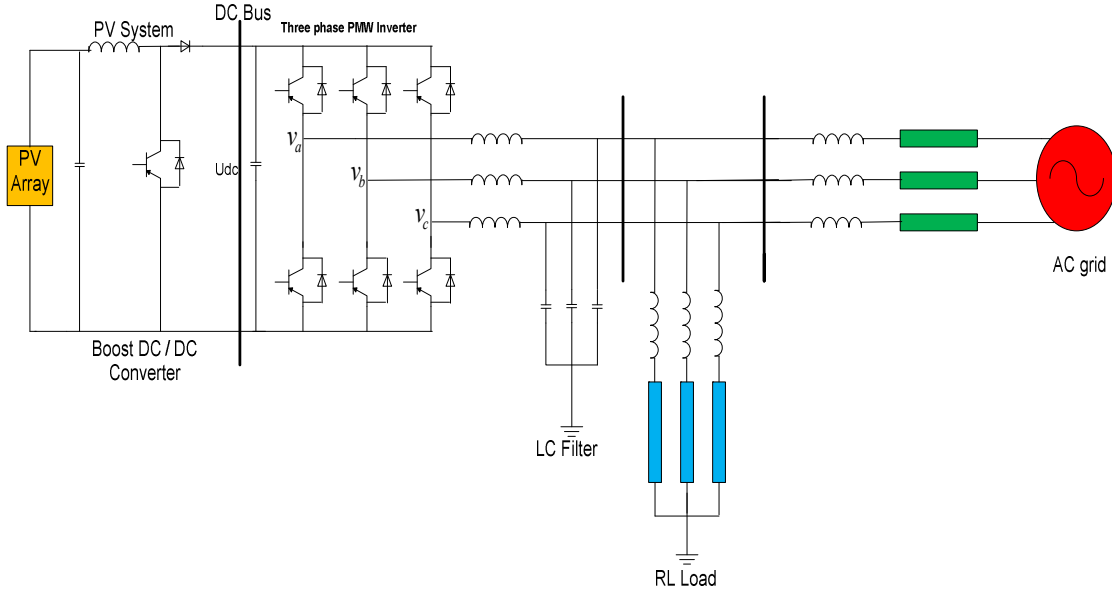


Figure1. The under study grid-connected photovoltaic generation system

**II. PHOTOVOLTAIC STRUCTURE**

A Photovoltaic generation is composed by many strings of solar cells in series, connected in parallel, in order to provide the desired values of output voltage and current. Figure 2 shows the equivalent circuit of a PV, from which nonlinear *I-V* characteristic can be deduced. Hence, the cells are connected in series and in parallel combinations in order to form an array with desired voltage and power levels. Applying Kirchoff's law of current, the terminal current of the cell is:

$$I = I_L - I_D \tag{1}$$

The light current is related to irradiance, temperature and the light current measured at some reference conditions:

$$I_L = \left( \frac{G}{G_{ref}} \right) \left[ (I_{L,ref}) + \mu_{I,sc} (T_c - T_{C,ref}) \right] \tag{2}$$

where  $I_{L,ref}$  is Light current at reference conditions [A],  $G$  and  $G_{ref}$  are the actual and reference irradiances [W/m<sup>2</sup>], respectively,  $T$  and  $T_{C,ref}$  are the actual and reference cell temperature [°K], and  $\mu_{I,sc}$  is manufacturer supplied temperature coefficient of short circuit current [A/°K]. The diode current is given by Shockley equation:

$$I_D = I_0 \left[ \exp \left( \frac{q(V + I_{RS})}{\gamma KTC} \right) - 1 \right] \tag{3}$$

where  $V$  is terminal voltage [V],  $I$  is reverse saturation current [A] and  $\gamma$  is shape factor,  $R_s$  is series resistance [Ω],  $q$  is electron charge  $1.602 \times 10^{-19}$  and  $K$  is Boltzmann constant,  $1.381 \times 10^{-23}$  J/K.

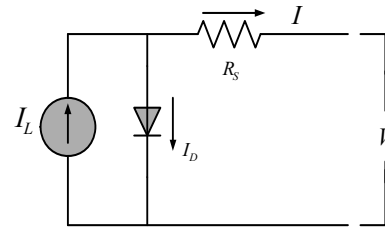


Figure 2. Solar cell equivalent circuit

The reverse saturation current is:

$$I_0 = D(T_c)^3 \exp \left( \frac{-q\varepsilon G}{AKT_c} \right) \tag{4}$$

where  $D$  is diode diffusion factor,  $\varepsilon G$  is material band gap energy (1.12 eV for Si, 1.35 eV for GaGs) and  $A$  is completion factor.

The reverse saturation current is actually computed by taking the ratio of Equation (4) at two different cell temperatures, thereby eliminating  $D$ , similar to the determination of  $I_L$ ,  $I_0$  is related to the temperature and the saturation current estimated at some reference conditions:

$$I_0 = I_{O,ref} \left( \frac{T_c}{T_{c,ref}} \right)^3 \exp \left[ \left( \frac{q\varepsilon G}{KA} \left( \frac{1}{T_{c,ref}} - \frac{1}{T_c} \right) \right) \right] \tag{5}$$

And thus the *I-V* characteristic is described by:

$$I = I_L - I_0 \left[ \exp \left( \frac{q(V + I_{RS})}{\gamma} \right) - 1 \right] \tag{6}$$

The shape factor  $\gamma$  is a measure of cell temperature and is related to the completion factor as:

$$\gamma = A.NCS.NS \tag{7}$$

where  $NCS$  is the number of cells connected in series per module.

A module is defined as an array of cells, usually encapsulated for protection, as it is supplied by manufacturer;  $NS$  is the number of modules connected in series of the entire array. While  $R_s$  and  $\gamma$  are assumed to be constant,  $I_L$  is a function of irradiance and cell temperature and  $I_o$  is a function of temperature only. The cell temperature can be determined from the ambient temperature and with the help of some standard test information. In [19] the way to evaluate these parameters based on the four model parameters proposed by Townsend [20], Eckstein [21] and Fry, Bryan [22] to be the most precised model that good produced the  $I-V$  characteristics.

Now only the four parameters  $I_L$ ,  $I_o$ ,  $R_s$  and  $\gamma$  need to be evaluated, a method to calculate these parameters has been developed by Eckstein. Since there are four unknown parameters, four conditions of the current  $I$  and the voltage  $V$  are needed. Generally, available manufacturer's information are set at three points at the reference conditions, ( $G = 1000 \text{ W/m}^2$ ,  $T = 25 \text{ }^\circ\text{C}$ ), the voltage at open circuit  $V_{OC,ref}$ , the current at short circuit  $I_{SC,ref}$  and the voltage and current at maximum power:  $V_{MP,ref}$  and  $I_{MP,ref}$ . The 4th condition comes from the knowledge of the temperature coefficients at short circuit:  $\mu I_{SC}$  and at open circuit:  $\mu V_{OC}$ .

$$I_{MP,ref} = I_{sc,ref} - I_{O,ref} \times \left( \exp V_t \cdot (V_{MP,ref} + I_{MP,ref} \times R_s) \right) \tag{18}$$

$$0 = I_{sc,ref} - I_{O,ref} \exp(V_t \cdot V_{OC,ref}) \tag{9}$$

$$I_{L,ref} \approx I_{sc,ref} \tag{10}$$

Substituting Equation (7) into Equation (9) and solving for  $\gamma$  and  $I_{O,ref}$  gives:

$$I_{O,ref} = I_{sc,ref} \cdot \exp(-V_t \cdot V_{OC,ref}) \tag{11}$$

$$\gamma_{ref} = \frac{q \cdot (V_{MP,ref} + R_s I_{MP,ref} - V_{OC,ref})}{K \cdot T_{c,ref} \cdot \ln \left( 1 - \frac{I_{MP,ref}}{I_{sc,ref}} \right)} \tag{12}$$

The indices  $OC$ ,  $SC$ ,  $MP$  and  $ref$  refer to the open circuit, the short circuit, the maximum power and the reference condition respectively. The cell's parameters change with the solar radiation  $G$  ( $\text{W/m}^2$ ) and ambient temperature  $T$  ( $^\circ\text{K}$ ) and they can be estimated by the following relations:

$$I_L = \left( \frac{G}{G_{ref}} \right) \left( I_{L,ref} + \mu_{Isc} (T_C - T_{c,ref}) \right) \tag{13}$$

$$I_O = I_{O,ref} \left( \frac{T}{T_{ref}} \right)^3 \exp \left( \frac{N_s E_q}{A} \right) \left( 1 - \frac{T_{c,ref}}{T_c} \right) \tag{14}$$

$$\gamma = \gamma_{ref} \left( \frac{T_c}{T_{c,ref}} \right) \tag{15}$$

The parameters evaluated in this section are based on the data for a single module at some reference condition. To describe the  $I-V$  characteristic for the entire array that contains series and parallel modules as shown in Figure 3.

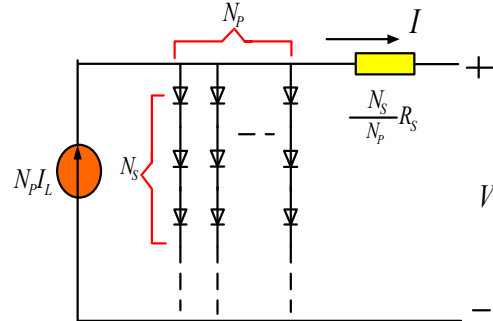


Figure 3. Mathematic model of a PV array

Parameters need to be scaled in the following way:

$$I_{L,tot} = N_p I_L \tag{16}$$

$$I_{O,tot} = N_p I_O \tag{17}$$

$$\gamma_{tot} = N_s \gamma \tag{18}$$

$$R_{s,tot} = \frac{N_s}{N_p} R_s \tag{19}$$

where,  $N_s$  and  $N_p$  are cell numbers of the series and parallel cells respectively. Connecting cells in series will increase the output voltage, and connecting them in parallel will increase the output current, corresponding to the expression (20) and (21):

$$I_{tot} = N_p I \tag{20}$$

$$V_{tot} = N_s V \tag{21}$$

All parameters of the model are valued based on the data in Table 1. Also output characteristics of PV array, with different temperatures and solar radiations, are presented in Figures 4 and 5.

Table 1. Parameters for PV Model

Parameters	Value
Number of cell use in series $N_s$	54
Referenced solar irradiance $G_{ref}$	1000 $\text{W/m}^2$
Referenced cell temperature $T_{ref}$	25 $^\circ\text{C}$
$I_{mp}$	7.629 [A]
$V_{mp}$	26.850 [V]
$P_{mp}$	204.857 [W]
$V_{oc}$	33.0978 [V]
$I_{sc}$	8.1887 [A]
$KV$	-0.1230 [KV]
$KI$	0.0032 [KA]

As shown in Figure 4 the PV cell represents nonlinear voltage-current characteristics, and there is only one point that makes the PV generator generating its maximum power under different environmental conditions.

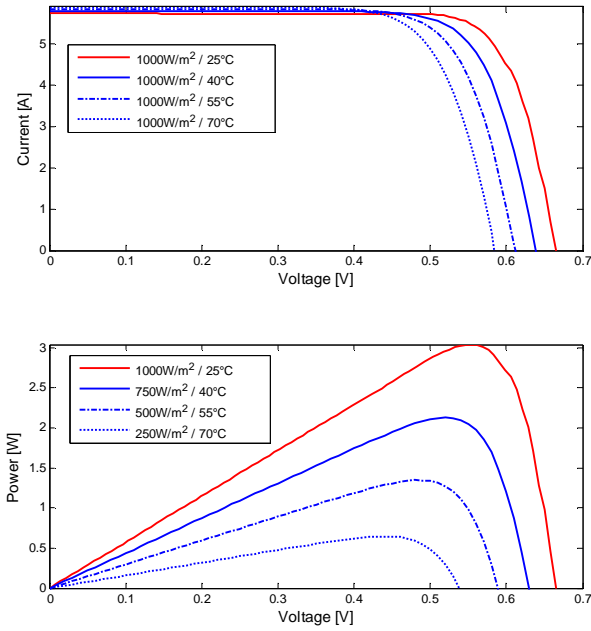


Figure 4. Effect of irradiance on  $I$ - $V$  characteristics and  $P$ - $V$  characteristics

### III. BOOST CIRCUIT AND ITS CONTROL

Since the output voltage of PV cell is low, the use of boost circuit will enable low-voltage PV array to be used, as a result, the total cost will be reduced. A capacitor is generally connected between PV array and the boost circuit, to reduce high frequency harmonics. Figure 5 shows the configuration of the boost circuit and its control system. The modeling of this converter depends on the analysis of the various sequences of operation whereas it has been supposed that durations fixed by a control element U. There are two sequences of operation depending on the state of the switch S, each one can be represented by a differential equation as explained in references [23, 24].

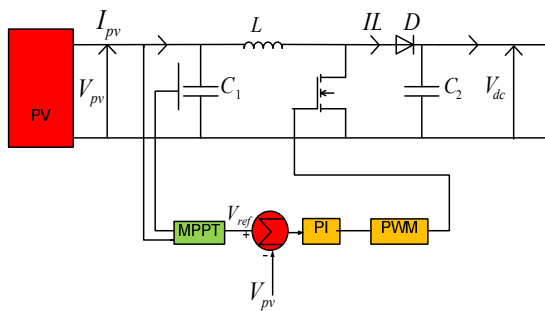


Figure 5. Boost circuit and its control

### IV. CONTROL OF THE GRID-CONNECTED INVERTER

PV array is connected to the ac grid via a common DC/AC inverter. The inverter is used in current control mode with PWM switching mechanism to make the inductance current track the sinusoidal reference current closely and obtain a low THD injected current.

#### A. Uncoupled Watt-VAR Method

In order to understand the principle of this method in the general case, we consider an inverter connected to the network, via a resistor  $R$  and inductance  $L$  (which represent the simplified model of a transformer), as indicated in Figure 6, which have the following equation [22]:

$$\frac{d}{dt} \begin{bmatrix} i_{g1} \\ i_{g2} \\ i_{g3} \end{bmatrix} - \begin{bmatrix} \frac{-R_g}{L_g} & 0 & 0 \\ 0 & \frac{-R_g}{L_g} & 0 \\ 0 & 0 & \frac{-R_g}{L_g} \end{bmatrix} \begin{bmatrix} i_{g1} \\ i_{g2} \\ i_{g3} \end{bmatrix} = \frac{1}{L_r} \begin{bmatrix} V_{g1} - e_1 \\ V_{g2} - e_2 \\ V_{g3} - e_3 \end{bmatrix} \quad (22)$$

where  $V_g$  and  $I_g$  represent the voltage and current of the grid,  $R_g$  and  $L_g$  are resistance and inductance of the grid and  $e$  is the inverter voltage. Applying the Park's abc to dq transformation, the Equation (22) is written in the following way:

$$\frac{d}{dt} \begin{bmatrix} i_{gd} \\ i_{gq} \end{bmatrix} - \begin{bmatrix} \frac{R_g}{L_g} & \omega \\ \omega & 0 \end{bmatrix} \begin{bmatrix} i_{gd} \\ i_{gq} \end{bmatrix} = \frac{1}{L} \begin{bmatrix} V_{gd} - e_d \\ V_{gq} - e_q \end{bmatrix} \quad (23)$$

To know the advantages of the control method, the traditional uncoupled Watt-VAR algorithm is briefly presented. Two new variables presented in (24), are the output variables of the control system which contains two PI controllers:

$$X_1 = \frac{1}{L_g} (V_{gd} - e_d) \quad , \quad X_2 = \frac{1}{L_g} (V_{gq} - e_q) \quad (24)$$

The values of  $i_{d,ref}$  and  $i_{q,ref}$  are the references of the active and reactive currents:

$$X_1 = \left( K_P + \frac{K_I}{S} \right) (I_{d,ref} - i_{gd}) - \omega i_{gq} \quad (25)$$

$$X_2 = \left( K_P + \frac{K_I}{S} \right) (I_{q,ref} - i_{gq}) - \omega i_{gd}$$

Applying the Laplace transformation to the Equations (23), (24) and (25) we obtain the transfer function as (26):

$$F(S) = \frac{i_{gd}}{i_{d,ref}} = \frac{i_{gq}}{i_{q,ref}} = \frac{K_I + SK_P}{K_I + S \left[ \frac{R_g}{L_g} + K_P + S^2 \right]} \quad (26)$$

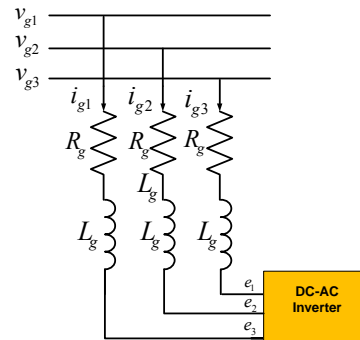


Figure 6. Diagram of an inverter connected to the grid

The diagram of control by the method “uncoupled Watt-VAR method” is represented in Figure 7. The complete block diagram of the identification of the references and regulation of the current for this method is shown on Figure 8, where the regulators are those of Figure 7. The goal of this control method is to impose the values of the active and reactive powers injected into electrical grid.

The powers at the point of connection are calculated in the dq reference frame [25]:

$$P_{ref} = \frac{3}{2}(V_{dr}i_{dr} + V_{qr}i_{qr}) \tag{27}$$

$$Q_{ref} = \frac{3}{2}(V_{dr}i_{qr} - V_{qr}i_{dr})$$

where  $P_{ref}$  and  $Q_{ref}$  are the reference powers. We can deduce the current in the dq frame as follows:

$$i_{d,ref} = \frac{2}{3} \frac{(P_g V_{gd} + Q_g V_{gq})}{V_{gd}^2 + V_{gq}^2} \tag{28}$$

$$i_{q,ref} = \frac{2}{3} \frac{(P_g V_{gq} - Q_g V_{gd})}{V_{gd}^2 + V_{gq}^2}$$

where  $V_{gd}$  and  $V_{gq}$  are the direct and quadrature components of the voltage at the connection point in the dq reference frame.

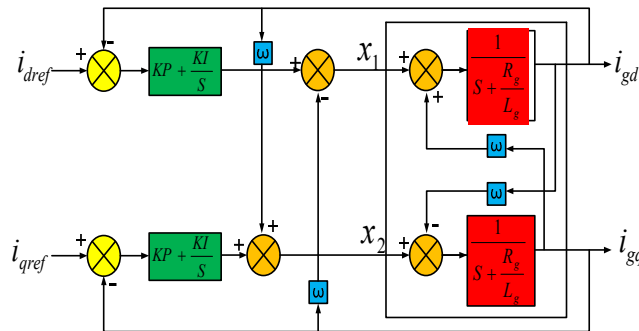


Figure 7. Block diagram of the uncoupled Watt-VAR control method

The  $i_{d,ref}$  and  $i_{q,ref}$  are the direct and quadrature current components injected into the grid. These currents depend on the power requested and the voltages measured at the point of connection. This voltage is transformed in the dq frame before the calculation of the currents as explained by Figure 8.

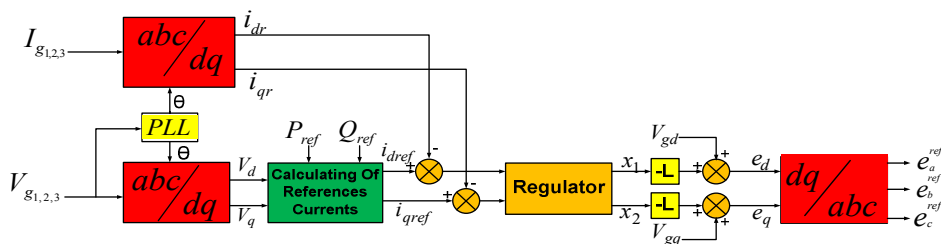


Figure 8. Complete Block diagram of control by the uncoupled Watt-VAR method

The role of the phase locked loop is to provide the rotation frequency, direct and quadrature voltage components at the point of common coupling (PCC) by resolving the grid voltage abc components. Multiple control blocks of the PV system rely on this information to regulate their output command signals. As stated earlier, the PLL computes the rotation frequency of the grid voltage vector by first transforming it to the dq frame, and then force the quadrature component of the voltage to zero to eliminate cross coupling in the active and reactive power terms [26].

A proportional-integral controller is used to perform this task. The proportional ( $K_p$ ) and integral ( $K_i$ ) gains of the controller were set through an iterative process to achieve a fast settling time. The components of the current are compared with its references. The differences between them passed through regulators, which give the components of the reference voltage in the dq reference. While passing by the reverse transformation dq to abc, we obtain the references of the PWM signals for the inverter.

**B. DC Bus Voltage Controller**

The regulation of this voltage is carried out when absorbing or providing the active power to the grid. The correction of this voltage must be done by the addition of an active fundamental current into the reference currents. Based on a difference between ( $U_{dc,ref}^2$ ) and ( $U_{dc}^2$ ), the power ( $P_{ref}$ ) on the regulator output side is added to the fluctuating active power and placed to an active fundamental current thus regulating the dc bus voltage. In order to obtain the ( $P_{ref}$ ) signal, we have the choice between a proportional regulator and a proportional-integral regulator. This last one is often used and gives better results in preventing the static errors. The schematic diagram of calculating and regulating of the DC bus voltage is shown in Figure 9.

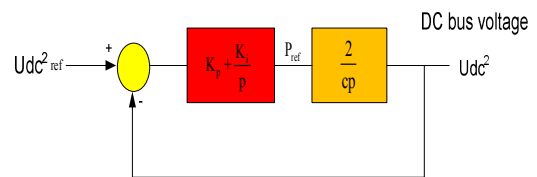


Figure 9. Schematic diagram of the DC link controller

**V. SIMULATION RESULTS**

Based on the above models and control methods, two simulation cases are studied:

- a. Steady operation, when there is no change in atmospheric conditions.
- b. Changes of solar irradiance and the dc bus control will stabilize the inverter input voltage.

**A. Steady State Operation**

When the system is in steady state, solar irradiance is 1000 W/m<sup>2</sup>, and the temperature is 298 °K.

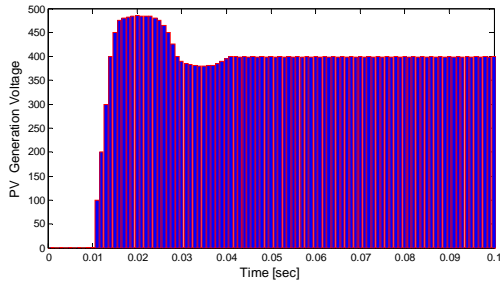


Figure 10(a). Photovoltaic generation voltage

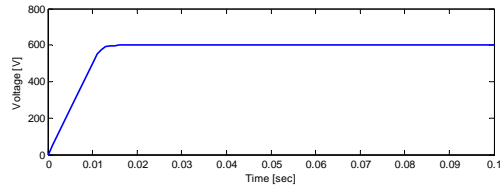


Figure 10(b). DC bus voltage

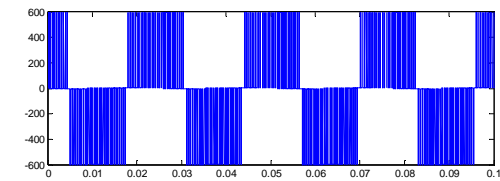


Figure 10(c). Phase to phase inverter's voltage before filtering

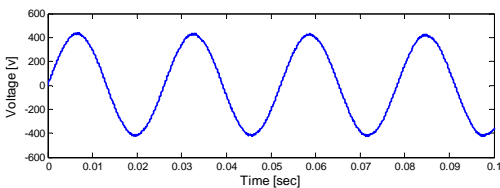


Figure 10(d). Phase to phase inverter's voltage after filtering

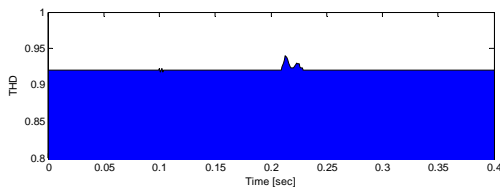


Figure 10(e). THD of voltage before filtering

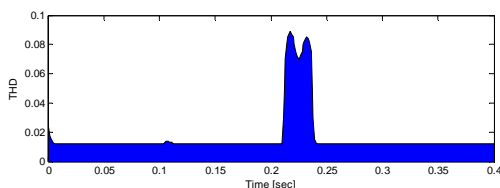


Figure 10(f). THD of voltage after filtering

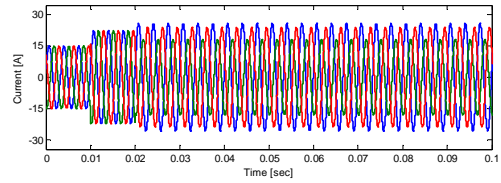


Figure 10(g). Inverter output currents

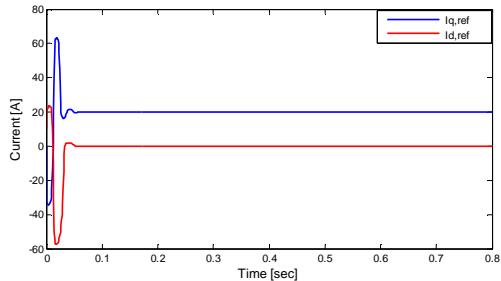


Figure 10(h).  $I_d$  and  $I_q$  reference currents

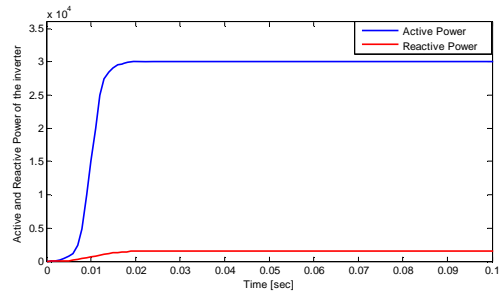


Figure 10(i). Active and reactive power of the inverter

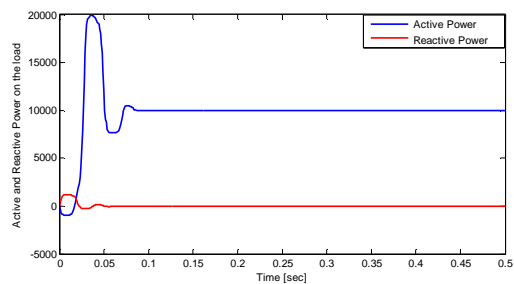


Figure 10(j). Active and reactive power of the load

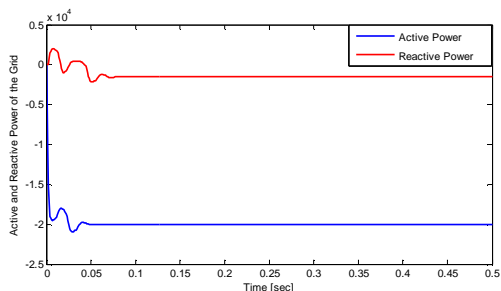


Figure 10(k). Active and reactive power of the grid

From Figures 10(a)-10(d), at this operation situation. In steady state, the operation point of PV array is just its maximum power point. The power requested by the load is 30 KW and 1 KVAR. Since the PV array generates only an active power of 10 KW and no reactive power (because the regulation system as shown in Figure 1 has two inputs  $I_{d,ref}$  and  $I_{q,ref}$  that is the image of reactive power and obviously its value is set to Zero) the rest of

the requested power comes from the grid as illustrate in Figures 10(i), 10(j), 10(k). The voltage at DC bus is regulated to be 600V the where currents of inverter have sinusoidal forms and its maximum is 20 A. Figures 10(c), 10(d), 10(e), 10(f) represents the voltage of the inverter before and after filtering. It seems that the filter has improved the THD from about 92 % into less than 1.35%.

**B. Changes of Solar Irradiance**

Assuming solar irradiance changes: during 0 to 0.01 sec, solar irradiance is 1000 W/m<sup>2</sup>; during 0.01 sec to 0.02 sec, solar irradiance is 500 W/m<sup>2</sup>; during 0.02 sec to 0.1 sec, solar irradiance returns to 1000 W/m<sup>2</sup>. Due to this change we have droop in both PV voltage and DC bus voltage as shown in Figures 11(a) and 11(b).

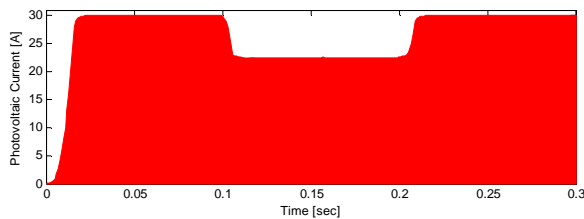


Figure 11(a). Photovoltaic current when solar irradiance changes from 1000 W/m<sup>2</sup> to 600 W/m<sup>2</sup> and then to 1000 W/m<sup>2</sup> again

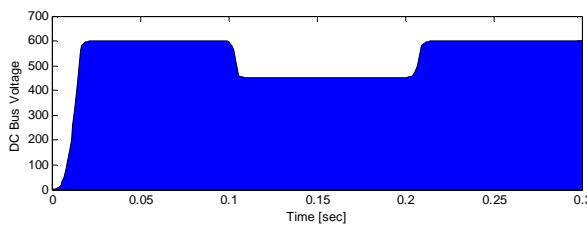


Figure 11(b). DC bus voltage when solar irradiance changes from 1000 W/m<sup>2</sup> to 600 W/m<sup>2</sup> and then to 1000 W/m<sup>2</sup> again

When solar irradiance is 600 W/m<sup>2</sup>, DC bus voltage is less than 600 V so the dc bus regulator must act to maintain the DC bus voltage constant (at 600 V). In figure 12 the DC bus voltage controller has insured a constant voltage that make PV system able to feed the inverter and the load.

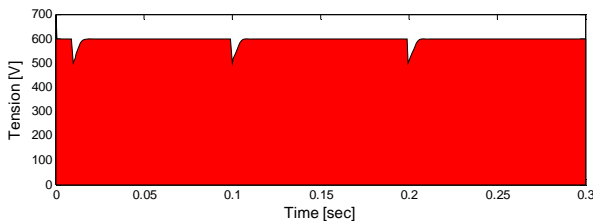


Figure 12. The effect of DC controller on the DC bus voltage

**VI. CONCLUSIONS**

This paper presents a three phase cascade inverter for grid connected photovoltaic systems. The proposed control strategy shows benefits for robust control against harmonic distortions in Photovoltaic system applications. The good performances of proposed strategy in both steady state and transient operation have been verified

through simulation results. In order to convert the solar energy efficiently, the maximum power point of the PV array should be tracked to ensure the PV array provides most power to both grid and the load. When solar irradiance or temperature fluctuates, PV generation will change as a result. The controller must act to maintain the DC bus voltage constant as possible and improve the stability of the whole system. The proposed control algorithm can bring several advantages such as follows:

- The system operates as a active filter capable of compensate harmonic components and reactive power, generated by the other loads connected to the system.
- Capability to supply AC loads and inject active power, from the photovoltaic system to the grid, relieving the grid demand (distributed generation).
- The MPPT technique is proposed to control the power between the grid and photovoltaic system, where it is intended to achieve the input voltage clamping operation.
- The proposed three phase PV system outweighs the conventional three phase PV systems, due to the lower THD index.
- The proposed control scheme makes the PV system capable to eliminate current harmonics as well as to compensate the reactive power load and to create symmetrical currents to the grid for balanced load.
- The inverter modules can be operating in parallel without line transformer isolation with utility grid since the current decoupling between inverter modules is implemented accurately by the proposed current-decoupling method. This will reduce the system cost.

The proposed control method has the ability to be used in other types of converters topologies and can be used for different types of renewable energy resources as power quality improvement devices in a custom power distribution grid. In addition, some simulation results were presented and they show theoretical viability of the proposed model, as well as the control strategy used for PV systems.

**REFERENCES**

[1] A. Jager Waldau, "Photovoltaics and Renewable Energies in Europe", Renewable Sustainable Energy Reviews, Vol. 11, No. 7, pp. 1414-1437, Sep. 2007.  
 [2] S. Rahman, "Green Power: What Is It and Where Can We Find It?", IEEE Power Energy Magazine, Vol. 1, No. 1, pp. 30-37, Jan./Feb. 2003.  
 [3] B. Bose, "Global Warming: Energy, Environmental Pollution, and the Impact of Power Electronics", IEEE Industrial Electronics Magazine, Vol. 4, No. 1, pp. 6-17, March 2010.  
 [4] B. Kroposki, R. Margolis, D. Ton, "Harnessing the Sun", IEEE Power Energy Magazine, Vol. 7, No. 3, pp. 22-32, May/June 2009.  
 [5] M. Liserre, T. Sauter, J.Y. Hung, "Future Energy Systems: Integrating Renewable Energy Sources into the Smart Power Grid through Industrial Electronics", IEEE Industrial Electronics Magazine, Vol. 4, No. 1, pp. 18-37, March 2010.

- [6] J.A. Gow, C.D. Manning, "Photovoltaic Converter System Suitable for Use in Small Scale Standalone or Grid Connected Applications", IEEE Proceeding of Electrical Power Applied, Vol. 147, No. 6, pp. 535-543, Nov. 2000.
- [7] M. Dali, J. Belhadj, X. Roboam, "Hybrid Solar-Wind System with Battery Storage Operating in Grid Connected and Standalone Mode: Control and Energy Management-Experimental Investigation Energy", Energy, Vol. 35, Issue 6, pp. 2587-2595, June 2010.
- [8] R.U. Ayers, H. Turton, T. Casten, "Energy Efficiency, Sustainability and Economic Growth", Energy, Vol. 32, Issue 5, pp. 634-648, May 2007.
- [9] C. Kahraman, I. Kaya, S. Cebi, "A Comparative Analysis for Multi-Attribute Selection among Renewable Energy Alternatives Using Fuzzy Axiomatic Design and Fuzzy Analytic Hierarchy Process", Energy, Vol. 34, Issue 10, pp. 1603-1616, Oct. 2009.
- [10] M.F. Akorede, H. Hizam, E. Pouresmaeil, "Distributed Energy Resources and Benefits to the Environment", Renewable Sustainable Energy Reviews, Vol. 14, Issue 2, pp. 724-734, Feb. 2010.
- [11] A. Bayod Rujula Angel, "Future Development of the Electricity Systems with Distributed Generation", Journal of Industrial Energy Efficiency, Vol. 34, Issue 3, pp. 377-383, Oct. 2009.
- [12] H. Lund, B.V. Mathiesen, "Energy System Analysis of 100% Renewable Energy Systems, the Case of Denmark in Years 2030 and 2050", Energy, Vol. 34, Issue 5, pp. 524-531, Feb. 2010.
- [13] A. Soroudi, M. Ehsan, "A Distribution Network Expansion Planning Model Considering Distributed Generation Options and Techno-Economical Issues", IEEE Transaction on Power System, Vol. 35, Issue 8, pp. 3364-3374, March 2010.
- [14] M. Abbas, J. Belhadj, A. Ben Abdelghani Bennani, "Design and Control of a Direct Drive Wind Turbine Equipped with Multilevel Converters", Journal of Renewable Energy, Vol. 35, Iss. 5, pp. 936-945, Apr. 2010.
- [15] F. Blaabjerg, R. Teodorescu, M. Liserre, V. Timbus Adrian, "Overview of Control and Grid Synchronization for Distributed Power Generation Systems", IEEE Transaction on Power Electronic, Vol. 53, Issue 5, pp. 1398-1409, Oct. 2006.
- [16] A. Rostami, K. Abbasian, N. Gorji, "Efficiency Optimization in a Rainbow Quantum Dot Solar Cell", International Journal on Technical and Physical Problems of Engineering (IJTPE), Issue 7, Vol. 3, No. 2, pp. 106-109, June 2011.
- [17] M. Sojoudi, R. Madatov, T. Sojoudi, "Optimization of Efficiency of Solar Cells by Accelerated Electron Ray to Have an Optimal and Constant Energy", International Journal on Technical and Physical Problems of Engineering (IJTPE), Issue 9, Vol. 3, No. 4, pp. 68-71, December 2011.
- [18] M.G. Simoes, F. Schetti, N.N. Arisc, "A Risc-Microcontroller Based Photovoltaic System for Illumination Applications", IEEE Applied Power Electronics Conference, Vol. 21, No. 4, pp. 1390-1406, June 2000.
- [19] R. Chenni, M. Makhlof, T. Kerbache, A. Bouzid, "A Detailed Modelling Method for Photovoltaic Cell", Journal of Industrial Energy Efficiency, Vol. 32, Issue 9, pp. 1724-1730, Sept. 2007.
- [20] A. Townsend, U. Timothy, "A Method for Estimating the Long-Term Performance of Direct-Coupled Photovoltaic Systems", M.Sc. Thesis. Solar Energy Laboratory, University of Wisconsin, Madison, Feb. 1989.
- [21] E. Jurgen Helmut, "Detailed Modeling of Photovoltaic Components", M.Sc. Thesis Solar Energy Laboratory, University of Wisconsin, Madison, 1990.
- [22] F. Bryan, "Simulation of Grid-Tied Building Integrated Photovoltaic Systems", M.Sc. Thesis Solar Energy Laboratory, University of Wisconsin, Madison, April 1998.
- [23] M. Fadel, "A New Control Method for DC/AC Converter with Sinusoidal Current", Journal of Industrial Energy Efficiency, Vol. 16, Issue 7, pp. 312-326, Oct. 2001.
- [24] V. Fernao Pires, "A Grid Connected Photovoltaic System with a Multilevel Inverter and a Le-Blanc Transformer", International Journal of Renewable Energy Research, V. Fernao Pires et al., Vol. 2, No. 1, Feb. 2012.
- [25] L. Ma, X. Jin, T. Kerekes, M. Liserre, R. Teodorescu, P. Rodriguez, "The PWM Strategies of Grid-Connected Distributed Generation Active NPC Inverters", IEEE Energy Conversion Congress and Exposition (ECCE '09), pp. 920-927, March 2009.
- [26] N. Kroutikova, C.A. Hernandez Aramburo, T.C. Green, "State Space Model of Grid-Connected Inverters under Current Control Mode", Electric Power Applications, IET, Vol. 1, No. 3, pp. 329-338, May 2007.

## BIOGRAPHIES



**Abolfazl Jalilvand** was born in Takestan, Iran in 1972. He received B.Sc. in Electrical and Electronic Engineering from Electrical and Computer Engineering Faculty, Shahid Beheshti University, Tehran, Iran, in 1995. He received M.Sc. and Ph.D. degrees from Electrical and Computer Engineering Faculty, University of Tabriz, Tabriz, Iran, in Power Engineering and Control Engineering in 1998 and 2005, respectively. After completing his Ph.D., he joined the Electrical Engineering Department, University of Zanjan, Zanjan, Iran, as an Assistant Professor where he was head of Electrical Engineering Department from 2008 to 2010. Also, he was Dean of Faculty of Engineering from 2010 to 2012. Currently, he is an Associate Professor at the same university. He has more than 110 papers in journals and conferences proceedings. His main research interests include the hybrid control systems, Petri nets, intelligent control, modeling and control of power electronic converters, control and stabilization of power systems, and application of intelligent methods in power systems. He is a member of the institute of electrical and electronics engineers (IEEE).



**Reza Noroozian** was born in Iran. He received the B.Sc. degree from University of Tabriz, Tabriz, Iran, in 2000, and the M.Sc. and Ph.D. degrees in Electrical Engineering from Amirkabir University of Technology, Tehran, Iran, in 2003 and 2008, respectively. Now he is an

Associate Professor with the Department of Electrical Engineering at University of Zanjan, Zanjan, Iran. His areas of interest include power electronics, power systems, power quality, integration and control of renewable generation units, custom power, micro grid operation, distributed-generation modeling, as well as operation and interface control.



**Mohsen Darabian** received his B.Sc. degree in Electrical Engineering from Abhar Branch, Islamic Azad University, Abhar, Iran, in 2010. He is currently a M.Sc. student at Department of Electrical Engineering, University of Zanjan, Zanjan, Iran. His research interests include

application of intelligent methods in power systems, distributed generation modeling, power electronics, FACTS, power quality and power system dynamics.